Clays and Clay Minerals, Vol. 47, No. 2, 144–155, 1999.

CHEMICAL CHANGES AND GENESIS OF SECONDARY MINERALS DURING THE ALTERATION OF BIOTITES FROM IGNIMBRITES IN THE TAZZEKA MOUNTAIN (MOROCCO)

JEAN DEJOU,[1] CHRISTIAN DE KIMPE,[2] JEAN-JACQUES MACAIRE,[3] AND ALAIN PERRUCHOT[4]

[1] 1, rue des Raux, 15250 Jussac, France
[2] Agriculture and Agri-Food Canada, Research Branch, Sir John Carling Building, 930 Carling Avenue, Ottawa, Ontario, Canada K1A 0C5
[3] EA 2100—Laboratoire de Géologie des Environnements Aquatiques Continentaux, Université François Rabelais, Parc de Grandmont, 37200 Tours, France
[4] EP CNRS 1748, Université de Paris-Sud, Bâtiment 504, 91045 Orsay Cedex, France

Abstract—The Tazzeka Mountain, located approximately 20 km south of Taza, eastern Morocco, is composed of a Westphalian volcano-sedimentary complex. It contains rhyolitic ignimbrites with the following minerals: quartz, potassium feldspar, oligoclase-andesine, and biotite. The ignimbrites are extensively altered because of a dense network of fractures in the massif. Alteration has resulted in the formation of spheroidal rocks and saprolite, the thickness of which depends on local topography. The evolution of the biotites in the ignimbrites was investigated by microprobe analysis of the mica crystals. This technique provides data that are not accessible through classical analytical methods. Biotites are transformed into secondary clay minerals, mainly chlorites and illites; intermediate stages are related to the degree of alteration of biotite, the latter being expressed by the K_2O content which decreases progressively from 7.3 to 1.3%. Next come protochlorites and chlorites *sensu stricto*, in which the K_2O content is 0.3%. Several processes including retrodiagenesis, hydrothermal activity, fumarolic activity, and geochemical weathering contributed to the transformation of the biotites at Tazzeka.

Key Words—Alteration, Biotite, Chlorite, Ignimbrite, Illite, Structural Formula.

INTRODUCTION

Alteration of biotites has been investigated by many authors who identified the major processes responsible for their evolution, including retrograde metamorphism below the weathering zone, hydrothermal activity and, weathering, in diverse geographical areas and under different climatic conditions, such as humid temperate, humid cold, humid Mediterranean, and humid tropical climates (Bisdom *et al.*, 1982; Chevalier, 1984; Parneix *et al.*, 1985; Dudoignon *et al.*, 1988). These authors stressed the importance of climatic conditions on the alteration of micas, and their evolution towards 2:1 and 1:1 phyllosilicates, interstratified secondary clay minerals, and even gibbsite under most intense leaching conditions.

The objective of this study is to provide further understanding of the chemical transformation of biotites under Mediterranean climate, more specifically by investigating the alteration of biotites in the ignimbrites from the Tazzeka Mountain, eastern Morocco. The focus of this study is on the nature of the alteration products, which differ considerably from site to site and with depth, and on the structural formulae of these secondary components.

GEOLOGICAL SETTING

The geological structure of the Tazzeka Mountain, a volcano-sedimentary complex located ~20 km south of Taza, eastern Morocco, was studied previously by Chalot-Prat (1986, 1990), Chalot-Prat and Cabanis (1989), Chalot-Prat and Galtier (1989), Chalot-Prat and Vachard (1989), Galtier *et al.* (1986), Huvelin (1986), and Robillard (1978). The complex occurs as outcrops at several locations, including the Khebbal Forest Station near Boujrada, at Bab-Bou-Idir and at Jorf-Bellout (Figure 1). At depth, an andesite complex, Upper Visean-Namurian in age, contains several facies: olivine-, amphibole-, and pyroxene-rich andesites, with labradorite as the most common plagioclase. Argillite-filled inclusions in the andesite contain plant remnants (Chalot-Prat and Galtier, 1989). The andesite complex is overlain by a Westphalian rhyolite-ignimbrite complex, the volume of which amounts to ~15 km^3, *i.e.*, about 65% of the 23 km^3 of the regional volcanic formations. The thickness of this complex varies from ~100–1000 m. It contains various xenoliths, *e.g.*, Ordovician schists, intravolcanic pyroclastic material, foraminifera-rich limestones, and magmatic rocks (basic and ophitic basalts). Red sandstones and tuffites cover the ignimbrites, followed by Keuperian red siltites and thick basaltic lava flows. Liassic dolomitic limestones are present at the top of this stratigraphic series.

Ignimbrites appear as rounded hills in the landscape. From a morphological view, they lie in a basin characterized by an extensive system of active and anas-

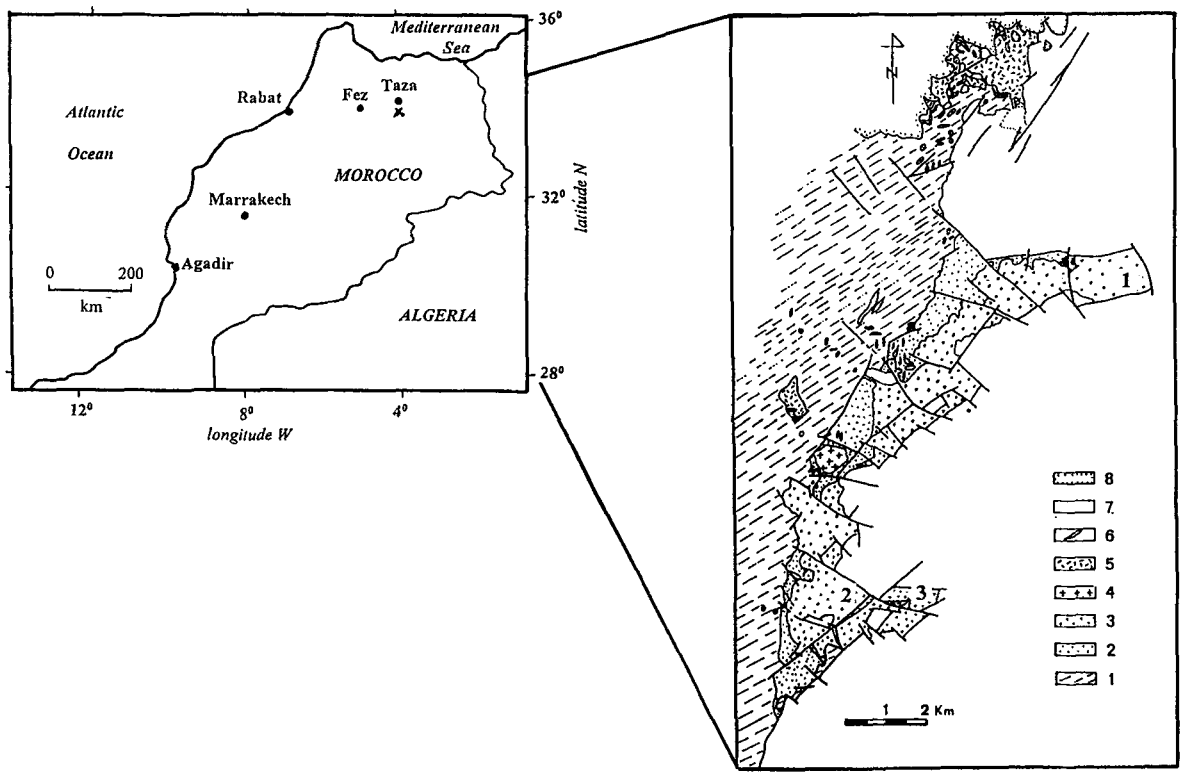

Figure 1. Location (x) of the study area in Morocco, and simplified geological map of the Tazzeka Volcanic Complex (after Chalot-Prat, 1986, 1990), showing also the sampling sites: Forest Station **(1)**, Jorf-Bellout **(2)**, and Bab-Bou-Idir **(3)**. Legend **(1)** basement; **(2)** andesite– and basalt-rich formation; **(3)** rhyolite- and ignimbrite-rich formation; **(4)** rhyolitic cumulodomes; **(5)** basic peripheric intrusions; **(6)** acid peripheric intrusions; **(7)** Mesozoic formation; **(8)** Miocene formation.

Table 1. Chemical analysis of Tazzeka ignimbrites.

Location: Element	Koudiat-Bouladayen	Bab-Bou-Idir	Jorf-Bellout[1]
SiO_2	65.00	64.04	73.89
Al_2O_3	14.40	15.30	13.35
TiO_2	0.54	0.85	0.38
Fe_2O_3	3.97	4.00	2.85
FeO	3.15	3.80	
MnO	0.16	0.23	0.10
P_2O_5	0.42	0.40	0.09
CaO	1.76	1.45	1.12
MgO	1.21	1.38	0.53
K_2O	4.84	4.38	4.24
Na_2O	1.15	2.70	2.19
H_2O^+	2.25	1.27	0.93
H_2O^-	0.03		
Cr_2O_3	0.14		
SO_3	0.21		
Cl_2O	0.03		
CuO	0.14		
BaO	0.27		
Total	99.68	99.80	99.67
Microcline/Plagioclase	1.78	0.94	1.06
Barytine (%)	0.48		
C.P.I.W. parameters	(I)II,3′,2,2[3′,1,1,3′]	(I)II,(3)4′,2,3[3,1,1,3(4)]	I,3,2′,3[4,1,1(2)3]
Nature of the rock	calco-alkaline rhyolite	calco-alkaline rhyolite	alkaline rhyolite

[1] After Chalot-Prat (1990).

https://doi.org/10.1346/CCMN.1999.0470204 Published online by Cambridge University Press

Table 2a. Mineralogical composition of Tazzeka ignimbrites (%).

Source	Koudiat-Bouladayen (KB)	Bab-Bou-Idir (BB 3)	Jorf-Bellout
Mineral			
Quartz	33.50	25.50	42.00
Potassium feldspar	29.70	26.90	24.10
Albite	—	—	22.60
Oligoclase-Andesine	15.30	27.00	—
Weathered biotite	—	—	3.50
Chlorite	10.80	12.30	—
Ilmenite	1.00	1.60	0.70
Fe hydroxide	2.50	1.60	2.20
Apatite	0.95	0.90	0.20
Residual Al_2O_3	2.65	1.70	3.30
$H_2O^+ + H_2O^-$	2.28	1.27	0.93
Total	98.68	98.77	99.53

Note: The mineral composition of the ignimbrites was calculated from the electron microanalyzer data, using structural formulae of the minerals.

tosmosed faults and fractures that have increased the rate of alteration of the ignimbrites, with the formation of spheroidal and ovoid rock masses, and of saprolite. Most saprolite is found *in situ,* except for that transported along some steep slopes. The color of the saprolite varies from site to site, ranging from gray to red. Thickness depends upon topography, between 0.5–5 m, and at some locations reaches 10 m.

MATERIALS AND METHODS

Samples

The following sites and samples were selected for this study (Figure 1):

1. At the Forest Station, an acid brown soil with A (0–25 cm) and AC (25–35 cm) horizons is developed on a reddish saprolite (35–135 cm) that covers the fractured ignimbrites. Samples FS 1, FS 2, and FS 3 were collected from the saprolite at depths of 35–60, 60–100, and 100–135 cm, respectively.
2. At Jorf-Bellout, the reddish ignimbrite is strongly altered into spheroidal and ovoid masses with an alteration cortex. This is a 0.5-m thick paleosaprolite; its development was restricted by the overlying Westphalian red sandstones and tuffites, Triassic red siltites and basalts, and Liassic dolomitic limestones. Sample JB 1 was obtained from the loose reddish saprolite.
3. At Bab-Bou-Idir, southwest of Tazzeka and at an elevation of 1510 m, ignimbrites are strongly altered to a depth of 10–15 m. The structure of the rock has disappeared, but several features, including fractures, spheroidal masses, and saprolite, are distinguishable. Samples were collected from top to bottom in the saprolite from three locations: (*a*) at 3–4 m below the surface (BB 1), in compact spheroidal rock fragments with an alteration cortex; (*b*) at 7–8 m below the surface (BB 2), in the disintegrated reddish saprolite; and (*c*) at the bottom of the saprolite (BB 3), in the fresh ignimbrite.
4. At Koudiat-Bouladayen, a sample was collected in the fresh ignimbrite.

Methods

The intermediate phases, from biotite through its alteration products, were characterized using the Tazaki and Fyfe (1987) method for describing the stages of K-feldspar alteration. The following techniques were used:

1. Samples were dispersed in 1 M NaOH solution, a strong dispersing agent, and the clay-size fraction (<2 μm) was obtained by sedimentation.
2. X-ray diffraction (XRD) analysis was performed on the <2 μm clay fraction, with the following treatments: original sample, glycerol-solvation, K-saturation at 25°C, and after heating at 300 and 500°C (McKeague and De Kimpe, 1978).
3. Total chemical analysis of fresh and altered rock samples, and of the alteration products was performed following fusion of the sample mixed with Sr-metaborate in an induction furnace, and dissolution of the fusion products in HNO_3. Analysis of the solution was then performed using atomic absorption spectroscopy.
4. Thin sections were examined under a polarizing microscope.

Table 2b. Structural formulae (KB and BB 3).

	K-feldspar			Plagioclase			Ferriferous chlorite		
	Si	12.00	Z = 15.95	Si	10.75	Z = 16.000	Si	5.72	8.000
	Al	3.95		Al	5.25		Al	2.28	
	Mg	tr		Fe	0.019		Al	2.72	
	Ca	0.025		Ca	1.246		Ti	0.006	
	Na	0.222	X = 4.097	Na	2.445	X = 3.941	Fe	5.64	
	K	3.850		K	0.231		Mn	0.12	
							Mg	3.22	11.762
Mol.	Or	94.0			5.9		Ca	0.015	
%	Al	5.6			62.4		Na	0.017	
	An	0.4			31.7		K	0.030	

https://doi.org/10.1346/CCMN.1999.0470204 Published online by Cambridge University Press

Table 3. Transformation of biotites to chlorites (Forest Station). Average SiO_2, Al_2O_3, FeO, MgO, and K_2O content of the samples at different stages.

		SiO_2		Al_2O_3		FeO		MgO		K_2O	
Stage	N[1]	x[2]	σ[3]	x	σ	x	σ	x	σ	x	σ
1	1	39.90		26.40		14.01		4.04		7.26	
2	3	37.63	1.55	25.41	2.34	17.38	2.14	3.70	1.47	5.95	0.11
3	5	36.91	0.62	24.75	0.67	17.33	1.00	5.49	0.32	5.16	0.18
4	5	34.91	2.96	23.04	2.44	20.85	6.40	5.15	2.06	4.42	0.39
5	4	34.67	0.90	23.58	1.40	23.13	5.83	4.47	2.23	3.81	0.15
6	7	33.57	2.10	23.67	0.94	22.04	2.70	6.45	0.25	3.22	0.15
7	5	33.33	1.90	23.28	0.84	20.88	2.76	6.92	2.10	2.76	0.12
8	2	30.43	0.03	21.61	0.14	26.48	0.55	7.95	0.74	2.17	0.07
9	6	30.37	2.82	22.35	1.46	25.34	2.64	8.15	1.60	1.36	0.25

Total number of microanalyzer determinations: 38. All Fe is expressed as FeO.
[1] N = number of microanalyzer measurements at each stage. [2] x = average value. [3] σ = standard deviation.

5. Microprobe analysis of altered biotite crystals was performed on thin sections, from the center to the edges of the crystals. This technique allows spot analyses that cannot be obtained through classical wet-chemistry methods. All major elements were determined, except that Fe is expressed entirely as Fe^{2+}.
6. Water content in the fresh rock was determined on 1-g samples: H_2O^- from weight loss at 105°C, and H_2O^+ from weight loss at 1000°C.
7. Structural formulae of the alteration products of biotite were calculated from chemical data. Formulae are approximate because the amount of Fe(II) and Fe(III) in the octahedral sheet of the clay minerals could not be differentiated analytically. However, Fe(II) is often dominant in the chemical composition of chlorites (Deer *et al.*, 1964; Weaver and Pollard, 1973; Newman, 1987), and this form was used in the calculation of the structural formula of chlorites. On the contrary, Fe(III) is largely dominant in illites, with an average of 86.7% of total Fe (Weaver and Pollard, 1973) and this form was used in the calculation of the structural formula for illites.

RESULTS

Chemical and mineralogical composition of ignimbrites

Throughout the volcanic massif, ignimbrites are relatively homogeneous; in this massive, light to dark rock, phenocrysts up to 3 mm in size represent 20–40% of the total volume. Chemical analyses of ignimbrite rock samples collected at three different locations in the Tazzeka Mountain show the following (Table 1): The SiO_2 content amounts to 64–65 wt. % in two samples (Koudiat-Bouladayen and Bab-Bou-Idir), and is ~74 wt. % in the third (Jorf-Bellout). Comparable values for SiO_2 content were reported previously at other sites in the Tazzeka Mountain (Chalot-Prat, 1990). Al_2O_3 and K_2O contents do not vary considerably, much less than Fe_2O_3, FeO, MgO and Na_2O. These ignimbrites belong to the calcalkaline and alkaline rhyolites, the Na_2O content determining the nature of the plagioclase.

The mineralogical composition of the ignimbrite (Table 2a) and structural formulae of the constituent minerals (Table 2b) were determined. In thin sections, all minerals are pyroclastic. Subhedral quartz crystals are somewhat corroded and contain inclusions. Potassium feldspar, often perthite, is a major component. Plagioclases fall in the oligoclase-andesine range, and frequently contain secondary calcite and occasionally a small amount of sericite. Biotites are strongly altered; no fresh biotite is observed in thin sections, including those from the least-weathered ignimbrite samples. Hematite exudate is present in intragranular and grain-boundary fractures of the micas. Apatite and barite are present, and rod-shaped titaniferous crystals, leucoxene and rutile, are found in epitaxy on the (001) plane of altered micas. Glass is recrystallized as quartz and feldspars. Minerals are embedded in a vitroclastic material composed of pumice glass. These ignimbrites originate from the effusion of pyroclastic clouds resulting from the pulverization of a rhyolitic magma. The data are consistent with previously reported observations of Chalot-Prat (1990).

The alteration products

Forest station: altered biotites, protochlorites, and trioctahedral chlorites. In the three FS samples, the >2 μm fraction amounts to 15 to 20% of the whole soil; the <50 μm fraction decreases from 30% in the A horizon to 5% in the C horizon, whereas the 20–200 μm fraction increases from 30 to 52%, and the 200–2000 μm fraction, from 30 to 40%. X-ray diffractograms of the <2 μm fraction show a peak at 1.36 nm that persits after heating at 550°C and after glycerol solvation; chlorite is thus present. Microprobe analyses of biotites at different stages of alteration and collected at three levels in the saprolite, between 35–135 cm, indicate a complex evolution; several stages of alteration can be identified in the three FS samples:

https://doi.org/10.1346/CCMN.1999.0470204 Published online by Cambridge University Press

Table 4a. Structural formulae of secondary minerals, based on 22 oxygen atoms.

Stage	1		2		3		4	
Si	5.880	8.000	5.730	8.000	5.636	8.000	5.529	8.000
Al	2.120		2.270		2.364		2.471	
Al	2.456	5.131	2.281	5.381	2.081	5.606	1.822	5.781
Ti	0.011		0.027		0.027		0.056	
Fe	1.721		2.205		2.205		2.642	
Mn	0.050		0.023		0.036		0.037	
Mg	0.843		0.845		1.257		1.224	
Ca	—	1.392	—	1.172	—	1.021	—	0.973
Na	0.027		0.015		0.015		0.080	
K	1.365		1.157		1.006		0.843	
SiO_2/Al_2O_3 mol.ratio	2.57		2.52		2.54		2.57	
Charge:								
tetrahedral	−2.120		−2.270		−2.374		−2.471	
octahedral	+0.729		+1.070		+1.320		+1.440	
interlayer	+1.392		+1.172		+1.021		+0.973	

Stage 1. Reference Biotite Mineral. The choice of this reference mineral in the Tazzeka context is difficult because the polarizing microscope analysis indicates that fresh biotite crystals are not present. The least weathered biotite crystals show a lighter color, some loss of pleochroism, and an exudation of opaque ferruginous material along cleavage planes (Roubault *et al.,* 1963). Chemical composition (Table 3) differs according to the geological occurrence; however, biotite at stage 1 contains more Al_2O_3 and less FeO, MgO and K_2O than many fresh biotites from plutonic and metamorphic rocks (Deer *et al.,* 1964; Rimsaite, 1967). Hydration is also higher than in fresh micas.

Stages 2 to 7. Increasing Degree of Alteration of Biotites. Under alteration, biotite crystals exfoliate, yet keep their original shape. Color is shifting from brownish to light greenish as in chlorite. Pleochroism is evolving from moderate in the first stages to weak in the latter ones. The right extinction is often incomplete, and birefringence decreases (Roubault *et al.,* 1963). The crystallographic characteristics do not allow clear separation of the successive stages, but the chemical analyses, especially the K_2O content, show significant differences from stage to stage (Tables 3 and 4a):

1. A rapid decrease of K_2O content, from 7.26 wt. % at stage 1 to 2.76 wt. % at stage 7. The content is significantly different from stage to stage, four times at P = 0.01, and twice at P = 0.001 (where P is the probability level).
2. A slow decrease of SiO_2 and Al_2O_3 contents. These oxides are generally homogeneous within each stage, with variability coefficient values ranging from 0.1 to 3.0%.
3. An increase of FeO and MgO contents. Within each stage, values are less homogeneous than for SiO_2,

Table 4b. Structural formulae of protochlorites, based on 28 oxygen atoms.

Element/Stage	8		9	
Si	6.267	8.000	6.298	8.000
Al	1.733		1.702	
Al	3.503	11.286	3.750	11.135
Ti	0.113		0.026	
Fe	4.544		4.378	
Mn	0.092		0.075	
Mg	2.455		2.534	
Na	0.007		0.012	
K	0.572		0.360	
SiO_2/Al_2O_3 mol.ratio	2.40		2.31	
Fe/Fe + Mg	0.65		0.63	

Table 5. Average chemical composition and structure of ferriferous chlorites (Stage 10).

Element	x[1]	σ[2]	C.V.[3]	Structural formula, based on 28 oxygen atoms		
SiO_2	26.28	1.02	3.88	Si	5.678	8.000
Al_2O_3	20.75	1.2	5.78	Al	2.322	
TiO_2	0.46					
FeO	30.95	1.78	5.75	Al	2.951	11.650
MnO	0.50	0.11	22.0	Ti	0.074	
CaO	—			Fe	5.573	
MgO	8.86	0.64	7.22	Mn	0.090	
K_2O	0.19	0.16	84.2	Ca	—	
Na_2O	0.02			Mg	2.871	
				K	0.083	
Total	88.01			Na	0.008	
Fe/Fe + Mg					0.66	
SiO_2/Al_2O_3 mol.ratio	2.15					

N = 20 samples. All Fe is expressed as FeO.
[1] x = average. [2] σ = standard deviation. [3] C.V. = coefficient of variation.

https://doi.org/10.1346/CCMN.1999.0470204 Published online by Cambridge University Press

Table 4a. Extended.

5		6		7	
5.446	8.000	5.282	8.000	5.319	8.000
2.554		2.718		2.681	
1.805	5.949	1.665	6.158	1.689	6.189
0.030		0.039		0.024	
3.028		2.890		2.777	
0.032		0.042		0.043	
1.054		1.522		1.656	
—	0.791	—	0.659	—	0.566
0.027		0.012		0.003	
0.764		0.647		0.563	
2.50		2.41		2.43	
−2.554		−2.718		−2.681	
+1.733		+2.018		+2.091	
+0.791		+0.659		+0.566	

Al_2O_3 and K_2O (five out of 12 variability coefficient values are >20%).

4. A charge increase in tetrahedral and octahedral sheets (Table 4a), with a corresponding charge decrease in the interlayer position. The latter charge is very low at stage 7, and this is supported by the extensive removal of alkaline cations.
5. An increase of hydration, with values between 10–12% for (H_2O^+ + H_2O).

Stages 8 and 9. Protochlorites. These minerals are close to chlorites: light green color, clean exfoliation, weak birefringence, abundant exudation of opaque products with frequent inclusions of apatite. Chemical composition of protochlorites contrasts with that at the previous stages: SiO_2 content decreases, while FeO and MgO contents increase to values close to those found in chlorites (Tables 3 and 4b). K_2O content decreases further, but is still larger than in chlorites *sensu stricto* where it does not exceed 0.3 wt. % (Deer *et al.*, 1964; Rimsaite, 1967). SiO_2/Al_2O_3 molecular ratios are higher, whereas Fe/Fe+Mg ratios are comparable to the corresponding values at stage 10. Structural formulae are calculated on the basis of 28 oxygen atoms to reflect the relationship of these minerals with chlorites.

Stage 10. Ferriferous Chlorites (Table 5). This represents the final stage in the transformation of the biotites. The crystals are colorless to light green, with weak pleochroism and birefringence, weak first order polarization, Ng − Np ≠ 0.01. Chemical composition is dominated by FeO, the content of which is higher than at stages 8 and 9 (Table 3), with a corresponding decrease of SiO_2 and Al_2O_3. SiO_2, Al_2O_3, FeO and MgO contents are generally homogeneous. K_2O content is <0.2%. The average composition of 20 samples falls in the range of chamosite-brünsvigite in the diagram by Hey (1954) (Figure 2).

Bab-Bou-Idir: chlorites, illites, and interstratified phyllites. Ignimbrite with Alteration Cortex (BB 1). This sample represents an early stage in the alteration of the ignimbrites. XRD patterns of the <2 μm fraction show the presence of chlorites, characterized by a peak at 1.4 nm that is maintained after glycerol-solvation and heating at 550°C, and derived from the biotites identified under the microscope. Electron microprobe

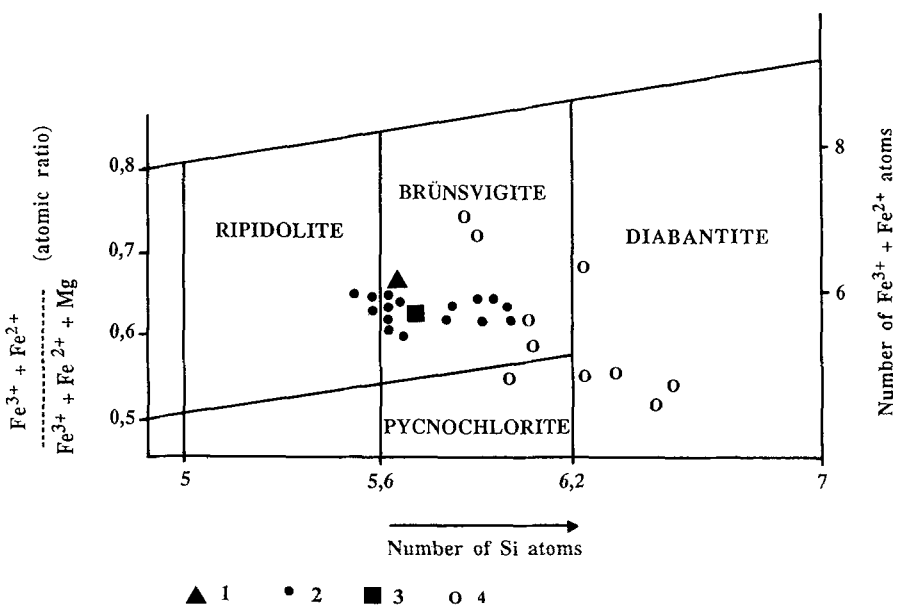

Figure 2. Position of chlorites in Hey's diagram: **(1)** average chemical composition of 20 ferriferous chlorites from the Forest Station; **(2)** chlorites from Bab-Bou-Idir; **(3)** average chemical composition of Bab-Bou-Idir chlorites; **(4)** Jorf-Bellout chlorites.

https://doi.org/10.1346/CCMN.1999.0470204 Published online by Cambridge University Press

Table 6. Average chemical composition of trioctahedral ferriferous chlorites. Ignimbrite with alteration cortex (BB 2).

Elements	x[1]	σ[2]	C.V.[3]	Structural formula, based on 28 oxygen atoms			Charge
SiO_2	25.92	0.74	2.85	Si	5.738	8.000	−2.26
Al_2O_3	19.17	0.54	2.82	Al	2.262		
TiO_2	0.04						
Cr_2O_3	0.01			Al	2.730		
FeO	30.58	1.37	4.48	Ti	0.006		
MnO	0.64	0.13	20.30	Cr	tr		
CaO	0.06			Fe	5.642		
MgO	9.70	0.33	3.40	Mn	0.120	11.781	+2.25
K_2O	0.11			Mg	3.221		
Na_2O	0.04			Ca	0.015		
				Na	0.017		
Total	86.27			K	0.030		
SiO_2/Al_2O_3	2.30			Fe/Fe + Mg[4]	0.64		

N = 16 samples. Measurements made in several parts of the crystals. Nature of the chlorite: brünsvigite.
[1] x = average. [2] σ = standard deviation. [3] C.V. = coefficient of variation. [4] All Fe is expressed as FeO.

analyses of 16 samples indicate that the chlorites are ferriferous, with a homogeneous composition (*i.e.,* small standard deviation and variability coefficient values for the major elements, SiO_2, Al_2O_3, FeO and MgO) (Table 6). These trioctahedral chlorites, with 5.5–6.1 Si atoms in tetrahedral position, 5.89 atoms in octahedral position and an interlayer occupancy of 0.03 cation, belong to the chamosite group (Melka, 1966) and are similar to the chlorites described by Wiewiora and Zeiss (1990). Crystallographic characteristics calculated from the chemical composition (Hey, 1954) *e.g.,* unit-cell parameters *a* and *b,* refractive index (ω), birefringence (ε − ω) and specific density D (Table 7), as well as their position in the diagram by Hey (Figure 2), further confirm the assignment. XRD patterns show that the cortex of this altered ignimbrite contains a small amount of illite.

Reddish Altered Ignimbrite (BB 2). The mineral assemblage, in addition to chlorite and illite, contains several other minerals:

1. 1.0–1.4 nm interstratified minerals characterized by XRD peaks at 1.21, 1.15, and 1.02 nm, that collapse to 1.0 nm upon heating. Electron microprobe analyses (Table 8) indicate that the minerals are trioctahedral, with an average octahedral occupancy of 5.5 cations, a SiO_2/Al_2O_3 molecular ratio of 2.84, moderate and high contents of K_2O and FeO, respectively, and high hydration. The negative charge in the tetrahedral sheet is high, and the interlamellar charge is +1.03, the same as in the octahedral position.
2. Dioctahedral illites (Table 9) with an average of 4.3 cations in the octahedral sheet. These minerals have low hydration, much less FeO, significantly higher (at P = 0.01) SiO_2 and Al_2O_3 contents, and a lower SiO_2/Al_2O_3 molecular ratio than the trioctahedral minerals, a low negative charge in the tetrahedral sheet, and a rather high charge in the interlayer position. Chemical composition of the K-bearing minerals is less homogeneous than in chlorites; only the SiO_2 and Al_2O_3 contents have variability coefficents <10%. Coefficients are much higher for the other constituents, to 44.7% for FeO. The Si-R2(FeO + MgO)-R3(Al_2O_3) diagram (Figure 3) illustrates the chemical composition variability of the K-bearing clay minerals.

Table 7. Characteristics of chlorites.

Sample	BB 2 (Table 6)	JF 1 (Table 10a)	JF 1 (Table 10b)
Nature of chlorites	Ferriferous chlorites	Fe-rich chlorite-brünsvigites	Pychno-chlorites-diabantites
Cell parameters (in nm)			
a	0.5367	0.5371	0.5353
b	0.9283	0.9281	0.9260
Refractive Index (ω)	1.632	1.636	1.609
Birefringence (ε-ω)	−0.001	−0.003	−0.001
Specific density (D)	3.04	3.07	2.91

Calculation from chemical composition of chlorites (after Hey, 1954).

Jorf-Bellout: a complex assemblage of secondary minerals. Ignimbrite Paleosaprolite, under Sandstone (JB 1). The mineral assemblage in the <2 μm fraction is more complex than in the samples from Bab-Bou-Idir. In addition to chlorites and illites characterized by XRD, the following minerals are identified by electron microprobe analysis:

1. Two groups of trioctahedral ferriferous chlorites: The first group (Table 10a) is characterized by high FeO and low Al_2O_3 contents; the chemical composition is homogeneous for the four samples analyzed. The second group (Table 10b) contains significantly less FeO (at P = 0.01) but more SiO_2 and MgO. The chemical composition is very homogeneous, with variability coefficients <7% for SiO_2,

https://doi.org/10.1346/CCMN.1999.0470204 Published online by Cambridge University Press

Table 8. Chemical composition of trioctahedral, Fe-rich K-phyllites. Reddish altered ignimbrite (BB 1).

Elements	x[1]	σ[2]	C.V.[3]	Sample with highest FeO content	Sample with lowest FeO content	Structural formula based on 28 oxygen atoms			Charge	
SiO_2	36.71	1.56	4.2	34.12	36.62	Si	5.857	8.000	−2.413	
Al_2O_3	21.95	1.93	8.8	22.70	24.30	Al	2.143			
TiO_2	0.02									
FeO	17.47	3.55	20.3	24.76	11.74	Al	1.977			
MnO	0.20	0.10	50.0	0.30	0.13	Ti	0.002			
CaO	0.37	0.06	16.2	0.40	0.30	Fe	2.232	5.561	+1.101	+2.140
MgO	5.15	0.81	15.7	4.71	3.72	Mn	0.027			
K_2O	4.36	0.68	15.6	5.11	3.25	Mg	1.233			
Na_2O	0.08	0.02	25.0	0.05	0.05					
						Ca	0.063			
Total	86.31			87.75	80.11	Na	0.025	0.976	+1.039	
						K	0.888			
SiO_2/Al_2O_3	2.84	0.22	7.7	3.26	2.56					

N = 11 samples. All Fe is expressed as FeO.
[1] x = average. [2] σ = standard deviation. [3] C.V. = coefficient of variation.

Al_2O_3, FeO and MgO. The tetrahedral charge and the SiO_2/Al_2O_3 molecular ratio are lower than in the first group. Some crystallographic characteristics, such as unit-cell parameters *a* and *b*, refractive index (ω), birefringence (ε − ω) and specific density D, calculated from the chemical data, are given in Table 7.

2. Dioctahedral illites: These minerals contain more FeO and K_2O than those from Bab-Bou-Idir (Table 11); the SiO_2/Al_2O_3 molecular ratio, 3.18 compared to 2.57, is significantly larger (at P = 0.001), as well as the positive charge in the interlayer position. These illites have a homogeneous chemical composition, as shown by the small dispersion of the representative points in the Si-R2-R3 diagram (Figure 4).
3. An illite, rich in FeO and low in Al_2O_3 and K_2O: It has a SiO_2/Al_2O_3 molecular ratio of 3.52, and a very low degree of substitution of Al for Si in the tetrahedral sheets (Table 12). The representative point for this mineral in the Si-R2-R3 diagram is closer to the Si pole, and distinct from the dioctahedral illites described above (Figure 4).
4. Secondary calcite: It is an almost pure (97.5%) component in four samples, with quartz as the complement. Homogeneity in composition (variability coefficient value of 0.70% for CaO) is noteworthy.

DISCUSSION AND CONCLUSIONS

Nature and origin of the secondary minerals

The dominant clay minerals in the <2 μm fraction resulting from the alteration of the ignimbrites are

Table 9. Chemical composition of dioctahedral, Fe-poor illites. Reddish altered ignimbrite (BB 1).

Elements	x[1]	σ[2]	C.V.[3]	Sample with highest (Fe total + K_2O) content	Sample with lowest (Fe total + K_2O) content	Structural formula based on 22 oxygen atoms			Charge	
SiO_2	47.17	0.86	1.82	46.63	48.43	Si	6.484	8.000	−1.516	
Al_2O_3	30.94	2.00	6.46	28.76	33.33	Al	1.516			
TiO_2	0.11			—	0.14					
Fe_2O_3	3.44			5.71	2.29	Al	3.478			
FeO	0.56			0.84	0.33	Fe(III)	0.353			
MnO	0.04			0.16	—	Fe(II)	0.064	4.241	+0.264	+1.458
CaO	0.22			0.20	0.20	Ti	0.011			
MgO	1.60	0.76	47.5	2.73	1.07	Mn	0.005			
K_2O	6.32	0.85	13.4	7.56	5.71	Mg	0.330			
Na_2O	0.08			0.06	0.04					
						Ca	0.032			
Total	90.48					Na	0.021	1.162	+1.194	
						K	1.109			
SiO_2/Al_2O_3	2.57	0.09	3.5	2.76						

N = 4 samples. Of the total Fe, 86% was taken as Fe(III), according to Weaver and Pollard (1973).
[1] x = average. [2] σ = standard deviation. [3] C.V. = coefficient of variation.

https://doi.org/10.1346/CCMN.1999.0470204 Published online by Cambridge University Press

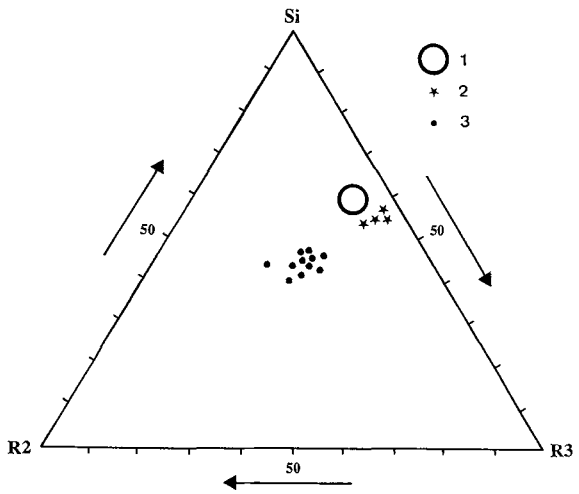

Figure 3. Chemical composition of Bab-Bou-Idir illites. R2 = FeO + MgO; R3 = Al_2O_3; (**1**) position of typical dioctahedral minerals; (**2**) dioctahedral illites, BB 1 site; (**3**) trioctahedral minerals, BB 1 site.

chlorites and illites. The same minerals were also identified in the alteration facies and related soils developed on volcanic ash and compact basalt (Dostal *et al.*, 1989; Shoji *et al.*, 1982), and these authors suggested that the chlorites and illites were derived from biotites. The same conclusion is inferred in the Tazzeka Mountain for the following reasons: (1) biotite is absent at Koudiat-Bouladayen and Bab-Bou-Idir whereas chlorite is a major component; (2) fresh biotite crystals were not found in any of the ignimbrites examined. Deer *et al.* (1964) suggest that the presence of FeO in biotite facilitates the alteration of this mineral; some FeO was assigned to this mica; and (3) except for biotite, the ignimbrites contain no ferromagnesian minerals that could transform into chlorite.

The susceptibility of biotite to alteration prevents calculation of the structural formula of biotite in its original condition. The nature of the secondary clay minerals resulting from the alteration of the biotites, their chemical composition, and crystallographic structure vary with the degree of alteration of the ignimbrites:

1. At the Forest Station, several stages in the evolution of biotites to chlorites are characterized. A relation between degree of alteration and depth is ruled out by the presence of the same stages of alteration at all depths in the saprolite.
2. At Bab-Bou-Idir, the chlorites are generally homogeneous in composition and belong to the brünsvigite subgroup in the chamosite group of minerals. In the diagram by Hey (1954) (Figure 2), 13 out of 16 chlorites fall in the brünsvigite domain, and three samples with a slightly lower SiO_2 content are in the ripidolite domain, yet very close to the brünsvigites.
3. The Jorf-Bellout chlorites are scattered in Hey's diagram. Some of them, with an average SiO_2/Al_2O_3 molecular ratio of 3.15 and a Fe/Fe+Mg ratio of 0.64, belong to brünsvigites. Others, with a higher SiO_2 content than brünsvigites and a Fe/Fe+Mg ratio of 0.50, belong to pycnochlorites-diabantites.

In the crystalline rocks from the Morvan, Seddoh (1973) found two types of chlorites, a primary chlorite formed in the retrodiagenesis zone and observed under the microscope in close association with altered biotite crystals, and a secondary chlorite formed in the saprolite and the soils. Although the possibility that two forms of chlorites exist at Tazzeka, it was not possible to distinguish such forms in this study. If two forms do exist, this would support a wide range of compositions.

Microsystems (Meunier, 1977) have a strong influence on the transformation of biotites at the three sites

Table 10a. Chemical composition of Fe-rich chlorite-brünsvigites (group I). Reddish ignimbrite under sandstone (JB 1).

Elements	x[1]	σ[2]	C.V.[3]	Sample with highest FeO content	Sample with lowest FeO content	Structural formula based on 28 oxygen atoms			Charge
SiO_2	24.29	1.52	6.2	23.02	23.64	Si	5.986	8.000	
Al_2O_3	13.20	1.55	11.7	11.17	14.26	Al	2.014		−2.014
TiO_2	0.09			0.24					
FeO	31.03	4.1	13.2	36.59	27.63	Al	1.813		
MnO	0.07				0.14	Ti	0.016		
Cr_2O_3	0.01				0.04	Cr	tr		
CaO	0.74			0.09	1.08	Fe	6.374		
MgO	9.84	0.58	5.9	9.04	10.22	Mn	0.015	12.116	
K_2O	0.13			0.30	0.08	Mg	3.638		
Na_2O	0.05			0.07	0.02	Ca	0.195		
						Na	0.024		
Total	79.45			81.12	77.11	K	0.041		+1.996
SiO_2/Al_2O_3	3.15	0.40	12.7	3.50	2.82	Fe/Fe+Mg	0.64		

N = 4 samples. All Fe is expressed as FeO.
[1] x = average. [2] σ = standard deviation. [3] C.V. = coefficient of variation.

https://doi.org/10.1346/CCMN.1999.0470204 Published online by Cambridge University Press

Table 10b. Chemical composition of pychnochlorite-diabantites (group II), (with less Fe than in group I). Reddish ignimbrite under sandstone (JB 1).

Elements	x[1]	σ[2]	C.V.[3]	Sample with highest FeO content	Sample with lowest FeO content	Structural formula based on 28 oxygen atoms			Charge
SiO_2	29.02	1.05	3.6	27.60	30.00	Si	6.277	8.000	−1.723
Al_2O_3	18.41	0.88	4.8	19.34	17.40	Al	1.723		
TiO_2	0.01								
FeO	22.94	0.98	4.3	24.33	21.52	Al	2.962		
MnO	0.18			0.20	0.05	Ti	0.001		
Cr_2O_3	tr			0.03		Cr	tr		
CaO	0.58			0.44	0.85	Fe	4.134		
MgO	12.62	0.86	6.8	12.30	13.58	Mn	0.032	11.401	+1.722
K_2O	0.11			0.03	0.12	Mg	4.094		
Na_2O	0.03			0.02	0.03	Ca	0.135		
						Na	0.013		
Total	83.90			84.29	83.63	K	0.030		
SiO_2/Al_2O_3	2.68	0.21	7.8	2.43	2.93	Fe/Fe + Mg	0.50		

N = 6 samples. All Fe is expressed as FeO.
[1] x = average. [2] σ = standard deviation. [3] C.V. = coefficient of variation.

investigated, namely the Forest Station, Bab-Bou-Idir and Jorf-Bellout. Although crystals appear homogeneous, differences in the chemical composition of secondary minerals are commonly found at the millimeter and even at the <0.1 mm scale: *e.g.*, in the BB 2 saprolite from Bab-Bou-Idir (7–8 m under the surface), several chlorites, and more or less altered products are observed within one <2 μm crystal. Differences in permeability and leaching conditions associated with the microfracture network determine different environments in the crystals. Even in crystals of small size, <0.1 mm, solutions circulate along preferential pathways and the duration of contact varies accordingly, thus resulting in a different evolution for each portion of the crystal (Glasmann and Simonson, 1985).

Illitization proceeds from the stage where ignimbrites develop an alteration cortex but before they transform to a saprolite (sample BB 2), to the stage where they are completely altered and exhibit a reddish colour (samples BB 1 and JF 1).

In contrast with observations made in the Beni-Toufout Massif, in northeastern Algeria (Penven *et al.*, 1981), and in Beaver County, Utah (Stringham, 1964), no transformation of biotites into kaolinite was detected at the sites under study. The absence of kaolinite is due to the relatively high base content of the parent rock (Table 1), and to the topogaphy: the mean slope from Jbel Tazzeka (at 1980 m) to the surrounding plains (at 500 m) and the city of Taza, 20 km away from the mountain, is 7.5%. However, close to the mountain, the

Table 11. Chemical composition of dioctahedral illites. Reddish ignimbrite under sandstone (JB 1).

Elements	x[1]	σ[2]	C.V.[3]	Sample with highest total Fe content	Sample with lowest total Fe content	Structural formula based on 22 oxygen atoms				Charge
SiO_2	48.52	1.83	3.8	45.70	51.00	Si	6.681	8.000	−1.319	
Al_2O_3	26.03	1.76	6.8	24.84	28.37	Al	1.319			
TiO_2	0.08			0.15	0.02					
Cr_2O_3	0.01			0.04		Al	2.897			−1.700
Fe_2O_3	6.22	2.27	34.8	10.50	4.50	Ti	0.008			
FeO	1.02			1.26	0.58	Cr	tr			
MnO	0.04			—	0.09	Fe(III)	0.642	4.036	−0.381	
CaO	0.15			0.28	—	Fe(II)	0.117			
MgO	1.78	0.17	9.6	1.88	1.62	Mn	0.008			
K_2O	9.31	0.60	6.4	9.34	9.02	Mg	0.367			
Na_2O	0.06			0.11	0.06					
						Ca	0.020			
Total	93.22			94.10	95.26	Na	0.016	1.671	+1.691	
						K	1.635			
SiO_2/Al_2O_3	3.18	0.11	3.5	3.13	3.06					

N = 7 samples. The difference of 0.61 in the SiO_2/Al_2O_3 ratio, with respect to the dioctahedral illites (BB 1) from Bab-Bou-Idir (Table 9) is highly significant (at P = 0.001).
[1] x = average. [2] σ = standard deviation. [3] C.V. = coefficient of variation.

https://doi.org/10.1346/CCMN.1999.0470204 Published online by Cambridge University Press

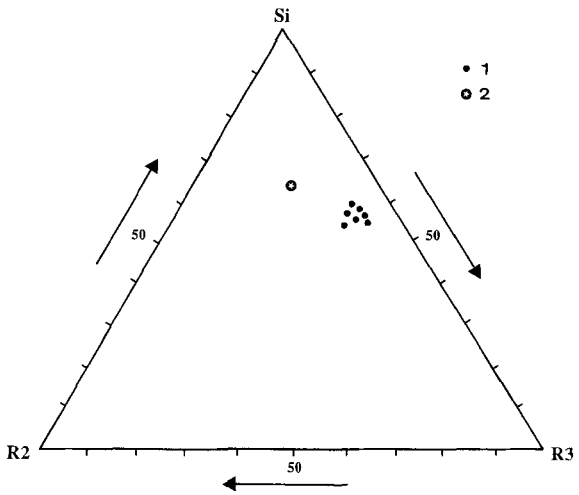

Figure 4. Composition of Jorf-Bellout illites: R2 = FeO + MgO; R3 = Al_2O_3; (**1**) dioctahedral illite; (**2**) Fe-rich illite.

Table 12. Chemical composition of a Fe-rich, Al-poor illite. Reddish ignimbrite under sandstone (JB 1).

Elements	%	Structural formula based on 22 oxygen atoms			Charge	
SiO_2	42.41	Si	6.992	8.000	−1.008	
Al_2O_3	10.23	Al	1.008			
TiO_2	0.30					
Fe_2O_3	20.83	Al	0.976			
FeO	3.39	Ti	0.037			
MnO	—	Fe(III)	2.576			
CaO	0.17	Fe(II)	0.466	4.290	+0.169	+0.960
MgO	0.95	Mn	—			
K_2O	3.44	Mg	0.235			
Na_2O	0.03					
		Ca	0.029			
Total	81.75	K	0.724	0.762	+0.791	
		Na	0.009			

86% of total Fe is expressed as Fe(II).

slopes are steeper, and thus conducive to erosion that rejuvenates the material exposed to alteration. Both factors are limiting geochemical evolution.

Processes influencing biotite evolution at Tazzeka

Major evolution processes at the sites under study (Table 13) can be inferred from field observations. Hydrothermal and fumarolic activity are favored by the complex fracture network: hydrothermal activity is indicated by the impregnation of the rock by barite and/or hematite to great depths; barite, associated with fumaroles (Eitel, 1966), is found at the Forest Station. Some rocks, however, are only slightly or are not affected by this process, especially at a distance from the fractures along which the hot fluids circulated. Chemical composition of fumaroles was investigated by many authors. In the Nea Kameni/Santorin area, Butuzova (1966), Georgalas (1940), Georgalas and Papastamatiou (1951, 1953), and Schorin (1980) found a high concentration of CO_2 and SO_2 in the hot vapors, and proposed that H_2SO_4 was the major factor altering the rocks by modifying their chemical composition, in particular the Al_2O_3, Fe_2O_3, TiO_2 and K_2O contents. In Alaska, Kodosky and Keith (1995) found halide species, *e.g.*, chlorides and fluorides, in the vapor phase. These authors reported that high-temperature gases extensively altered the glass and mineral phases adjacent to the fumarolic conduit. When fumaroles cooled, aqueous chloride complexes became an important mechanism for element transport. Although it is difficult to ascertain whether hydrothermal activity was more important than fumarolic activity in the Tazzeka Mountain, hot fluids associated with hydrothermal activity are likely more efficient for the removal of cations, thus with a more global effect than fumarolic activity. Retrograde metamorphism likely occurred in the alteration of biotites, but was often masked by hydrothermal activity. Finally, weathering had its own effect down to a few meters below the soil surface, and controlled the general evolution, leading to the disintegration of ignimbrites and the formation of the spheroidal masses.

Calcite may have resulted from *in situ* alteration of the plagioclases in the ignimbrites, or from a reprecipitation from carbonate-rich solutions percolating from above, especially from the altered Triassic basalts or the Liassic dolomitic limestones.

Age of alteration of the ignimbrites

It is difficult to precisely define the age of this alteration. However, we believe that it is older than the

Table 13. Processes for the alteration of biotites at Tazzeka.

Site	Reference sample	Sample type	Hydrothermalism and/or fumarolic activity	Weathering
Forest Station	FS 1, 2, 3	saprolite (35–135cm)	++[2]	
	BB 3	parent rock	+[1]	
Bab-Bou-Idir	BB 2	saprolite (7–8m)	++	+
	BB 1	saprolite (3–4m)	+	+
Jorf-Bellout	FB 1	saprolite (0–50cm)	+	+

[1] + clear. [2] ++ very clear.

https://doi.org/10.1346/CCMN.1999.0470204 Published online by Cambridge University Press

Keuperian Sandstones, since the ignimbrite saprolite is covered by these sandstones at Jorf-Bellout. The alteration through the sandstones continued probably for some time later on. The genesis of the saprolite was terminated by weathering under quaternary climatic conditions.

REFERENCES

Bisdom, E.D.A., Stoops, G., Delvigne, J., Curmi, P., and Altemuller, H.J. (1982) Micromophology of weathered biotite and its secondary products. *Pédologie,* **32,** 225–252.

Butuzova, G.Y. (1996) Iron ore sediments of the fumarole field of Santorini volcano, their composition and origin. *Døklady Akademie Nauk SSSR,* **168,** 1400–1402.

Chalot-Prat, F. (1986) Mise en évidence d'une dépression volcano-tectonique associée à d'épais épanchments ignimbritiques hercyniens dans le Massif du Tazzeka (Maroc oriental). *Revue de Geologie Dynamique et de Geographie Physique,* **27,** 193–203.

Chalot-Prat, F. (1990) Pétrogenèse d'un volcanisme intracontinental tardi-orogénique hercynien. Etude du complexe volcanique carbonifère du Tazzeka et des zones volcaniques comparables dans le Mekam et la région de Jeradu (Maroc oriental). Thesis, Université de Pierre and Marie Curie, Paris, 300 pp.

Chalot-Prat, F. and Cabanis, B. (1989) Découverte dans les volcanites carbonifères du Tazzeka (Maroc oriental) de la coexistence de diverses séries basiques, d'une série acide et d'importants phénomènes de mélanges. *Comptes Rendus de l'Académie des Sciences de Paris, Série II,* **308,** 739–745.

Chalot-Prat, F. and Galtier, J. (1989) Découverte d'un tronc de gymnosperme dans une coulée du complexe volcanique carbonifère du Tazzeka (Maroc oriental) et sa signification paléoécologique. *Comptes Rendus de l'Académie des Sciences de Paris, Série II,* **309,** 1735–1741.

Chalot-Prat, F. and Vachard, D. (1989) Découvertes de Foraminifères serpoukhoviens (Namurien inférieur) dans la série volcano-sédimentaire du Tazzeka (Maroc oriental). *Comptes Rendus de l'Académie des Sciences de Paris, Série II,* **308,** 1157–1160.

Chevalier, Y. (1984) Altération météorique actuelle et paléoaltérations du socle provençal (France). Evolution comparée des roches et des eaux de lessivage cordrespondantes. Etude physico-chimique, mécanique, minéralogique et hydrogéochimique. Ph.D. thesis, Université de Nice, 691 pp.

Deer, W.A., Howie, R.A., and Zussman, J. (1964) *Rock-Forming Minerals. Volume 3, Sheet Silicates.* Longman, London.

Dostal, J., Jackson, G.D., and Galley, A. (1989) Geochemistry of neohelikian Nanynt plateau basalts, Border rift basin, northwestern Baffin Island, Canada. *Canadian Journal of Earth Sciences,* **26,** 2214–2223.

Dudoignon, P., Beaufort, D., and Galley, A. (1988) Hydrothermal and supergene alterations in the granitic cupola of Montebras, Creuse, France. *Clays and Clay Minerals,* **36,** 505–520.

Eitel, W. (1966) *Silicate Science. Volume 4. Hydrothermal silicate system.* Academic Press, New York, 617 pp.

Galtier, J., Phillips, T.L., and Chalot-Prat, F. (1986) Euramerican coal-swamp plants in mid-carboniferous of Morocco. *Review of Palaeobotany and Palynology,* **49,** 93–98.

Georgalas, G.C. (1940) Die postvulkanische Fumarolentätigkeit und der Wärmehaushalt des Santorin-Vulkans. *Bulletin of Volcanology, Series II,* **6,** 237–242.

Georgalas, G.C. and Papastamatiou, J. (1951) Über den Ausbruch des Santorin-Vulkans von 1939–1941. Der Ktenas-Ausbruch. *Bulletin of Volcanology, Series II,* **11,** 3–37.

Georgalas, G.C. and Papastamatiou, J. (1953) L'éruption du volcan de Santorin en 1939–1941. L'éruption du dôme Fouque. *Bulletin of Volcanology, Series II,* **13,** 3–38.

Glasmann, J.R. and Simonson, G.A. (1985) Alteration of basalt in soils of western Oregon. *Soil Science Society of America Journal,* **49,** 262–273.

Hey, M.H. (1954) A new review of chlorites. *Mineralogical Magazine,* **30,** 277–292.

Huvelin, P. (1986) Le Carbonifère du Tazzeka (Maroc). Volcanisme et phénomènes de resédimentation. *Comptes Rendus de l'Académie des Sciences de Paris, Série II,* **303,** 1483–1488.

Kodosky, L.G. and Keith, T.E.C. (1995) Further insights into the geochemical evolution of fumarolic alteration, Valley of Ten Thousand Smokes, Alaska. *Journal of Volcanic and Geothermal Research,* **65,** 181–190.

McKeague, J.A. and De Kimpe, C.R. (1978) *Manuel de méthodes d'échantillonnage et d'analyse des sols.* Canadian Society of Soil Science, Ottawa, 230 pp.

Melka, K. (1966) New suggestions for the subdivision of the chlorite group. *Proceedings of the International Clay Conference, Jerusalem,* **1,** 27–31.

Meunier, A. (1977) Les mécanismes de l'altération des granites et le rôle des microsystèmes. Etude des arènes du massif granitique de Parthenay (Deux-Sèvres). Ph.D. thesis, Université de Poitiers, 247 pp.

Newman, A. (1987) *The Chemistry of Clay and Clay Minerals. Monograph Number 6.* Mineralogical Society, London.

Parneix, J.C., Beaufort, D., Dudoignon, P., and Meunier, A. (1985) Biotite chloritization process in hydrothermally altered granites. *Chemical Geology,* **51,** 89–101.

Penven, M.J., Fedoroff, N., and Robert, M. (1981) Altération météorique des biotites en Algérie. *Geoderma,* **26,** 287–309.

Rimsaite, J.H.Y. (1967) Studies of rock-forming micas. *Geological Survey of Canada. Energy, Mines, and Resources Bulletin Number 149,* 82 pp.

Robillard, D. (1978) Etude structurale du Moyen Atlas septentrional (région de Taza, Maroc). Thesis, 3ième cycle. Université de Lille, 178 pp.

Roubault, M., Fabriès, J., Touret, J., and Weisbrod, A.A. (1963) *Détermination des minéraux des roches au microscope polarisant.* Lamarre-Poissat, eds., Paris, 365 pp.

Schorin, H. (von) (1980) Zersetzung von Kalk-Alkali-Gesteinen im rezenten Fumarolengebiet. *Geologische Rundschau,* **69,** 226–244.

Seddoh, F.K. (1973) Altération des roches cristallines en Morvan. Etude minéralogique, géochimique et micromorphologique. thesis, Fac. Sc. Dijon. Memoires geologiques de l'Université de Dijon. 377 pp.

Shoji, S., Fujiwara, Y., Yamada, I., and Saigusa, M. (1982) Chemical and clay mineralogy of andosoils, brown forest soils and podzolic soils formed from recent Towada ashes, northeastern Japan. *Soil Science,* **133,** 69–86.

Stringham, B. (1964) Hydrothermal alteration of ignimbrites, Beaver County, Utah. *Geological Society of America Special Paper,* **76,** 294.

Tazaki, K. and Fyfe, W.S. (1987) Primitive clay precursors formed on feldspar. *Canadian Journal of Earth Sciences,* **24,** 506–527.

Weaver, C.E. and Pollard, L.D. (1973) Developments in Sedimentology. *The Chemistry of Clay Minerals.* Elsevier, Amsterdam, 213 pp.

Wiewiora, A. and Zeiss, Z. (1990) Crystallochemical classification of phyllosilicates based on the unified system of projection of chemical composition. II. The chlorite group. *Clay Minerals,* **25,** 83–92.

(Received 11 March 1997; accepted 15 July 1998; Ms. 97-022)